Mechanical Systems and Signal Processing 102 (2018) 180–197

Contents lists available at ScienceDirect

Mechanical Systems and Signal Processing

journal homepage: www.elsevier.com/locate/ymssp

Review

Estimation of beam material random field properties via sensitivity-based model updating using experimental frequency response functions

M.R. Machado [a,*], S. Adhikari [b], J.M.C. Dos Santos [c], J.R.F. Arruda [c]

[a] Department of Mechanical Engineering, University of Brasilia – UnB, 70910-900 Brasilia, Brazil
[b] School of Engineering, Swansea University, Singleton Park, Swansea SA2 8PP, UK
[c] Department of Computational Mechanics, University of Campinas – UNICAMP, 13083-970 Campinas, SP, Brazil

ARTICLE INFO

Article history:
Received 31 May 2017
Received in revised form 19 August 2017
Accepted 24 August 2017

Keywords:
Parameter estimation
Sensitivity-based model updating
Random field

ABSTRACT

Structural parameter estimation is affected not only by measurement noise but also by unknown uncertainties which are present in the system. Deterministic structural model updating methods minimise the difference between experimentally measured data and computational prediction. Sensitivity-based methods are very efficient in solving structural model updating problems. Material and geometrical parameters of the structure such as Poisson's ratio, Young's modulus, mass density, modal damping, etc. are usually considered deterministic and homogeneous. In this paper, the distributed and non-homogeneous characteristics of these parameters are considered in the model updating. The parameters are taken as spatially correlated random fields and are expanded in a spectral Karhunen-Loève (KL) decomposition. Using the KL expansion, the spectral dynamic stiffness matrix of the beam is expanded as a series in terms of discretized parameters, which can be estimated using sensitivity-based model updating techniques. Numerical and experimental tests involving a beam with distributed bending rigidity and mass density are used to verify the proposed method. This extension of standard model updating procedures can enhance the dynamic description of structural dynamic models.

Contents

* Corresponding author.
E-mail address: mromarcela@gmail.com (M.R. Machado).

https://doi.org/10.1016/j.ymssp.2017.08.039
0888-3270/

1. Introduction

Quantifying uncertainty in numerically simulated results is not recent. However, during the last few years, this research area has undergone remarkable development, in special for dynamic systems. The method most used is Monte Carlo (MC) simulation [1]. Otherwise, non-sampling approaches such as the Perturbation Method may be used. It consists of expanding a random field in a truncated Taylor series around its mean [2]. The Direct Method consists in applying the moment equations to obtain the random solutions. The unknowns are the moments and their equations are derived by taking averages over the original stochastic governing equations. A powerful method in computational stochastic problems is the Stochastic Finite Element Method (SFEM) [3]. SFEM is an extension of the classical deterministic FE approach to the stochastic framework, i.e., to solve static and dynamic problems with stochastic mechanical, geometric, or loading properties [4]. Adhikari [5] presented a doubly Spectral Stochastic Finite Element Method, where the Spectral Element Method is given a stochastic treatment.

The spectral element method (SEM) [6,7] is based on the analytical solution of the displacement wave equation, written in the frequency domain. The element is tailored with the matrix ideas of FEM, but in SEM the interpolation function is the exact solution of the wave equation [8–20]. Both techniques, SFEM and doubly Spectral SFEM, are formulated in a context of random fields. A method with a wide application when considering random fields is the Karhunen-Loève (KL) expansion [3,21,2]. The KL expansion can be used to discretize the random field by representing it by scalar independent random variables and continuous deterministic functions. By truncating the expansion, the number of random variables becomes finite and numerically treatable. Many authors use the KL expansion to model Gaussian random processes, but it is possible to extend the KL expansion to non-Gaussian processes [22–25].

Model updating methods in dynamic structural analysis are basically a process of minimizing the differences between the numerical model predictions and measured responses obtained in experimental tests using a parameter estimation procedure [26,27]. The model updating procedure starts with the parameter choice (parametrisation), followed by a correction procedure based on the available measured data. The parametrisation is an important topic in model updating which requires considerable physical knowledge regarding the system. More details can be found in references [28–32]. In the field of structural dynamics, some authors traditionally use modal parameters (natural frequencies and mode shapes) for updating the model due to the facility in estimating the modal parameters using modal analysis [33,34] and also to the freedom in the choice of the updating parameters and the applicability of the method [35]. Examples of theoretical and practical applications can be found in references [36,27,37,38,32]. However, in a structural dynamic test, it is a common practice to measure the data in the form of Frequency Response Functions (FRF), which requires an additional modal parameter estimation [33,39] to extract the modal parameters. Natke [40] presented a model updating procedure using measured FRFs instead of modal parameters. After that, a growing number of researchers focused on model updating algorithms using the measured data directly [41–47]. In the practical applications of model updating, the measured data are often incomplete and include randomness. Based on the system variability, some authors proposed stochastic model updating techniques [48–51]. The main advantage of this approach is to add randomness in the model updating process. Statistical techniques combined with model updating can improve the parameter estimation. The first works that incorporated statistical methods for the treatment of measurement noise in model updating were presented by Collins et al.[52] and later by Friswell [53]. Differences between measure data and model predictions may arise due to randomness present in the system, e.g. manufacturing variability as well as to variations in the material properties of the structure components. In Friswell's paper [53], errors in the analytical model and in the measurements (e.g. caused by noise [27]) are associated to a weighting matrix and it is shown how to estimate the variance in the updated parameters. This technique is called the minimum variance estimator. Other techniques for model updating in the presence of uncertainty are the Bayesian probabilistic framework presented by Beck, Katafygiotis, and Mares [54–56], model updating based on an inverse approach, and fuzzy arithmetic [57]. Soize [58] presented a methodology for robust model updating using a non-parametric probabilistic approach. Uncertainty in structural properties, such as Poisson's ratio, Young's modulus, mass density, modal damping, etc., are considered irreducible uncertainty and require different mathematical approaches for the updating procedure. The distributions of the updated parameters are then modified in order to improve the correlation between model-predicted distributions and measured data distributions. This is a technique developed by Mottershead et al., and Mare et al. [59,56] and it is called stochastic model updating or uncertainty identification. The stochastic model updating is efficient, not only because it includes variability data due to measurement noise, for example, but also because it includes the variability already existing in the structural property [59,56,48–50]. Govers and Link [60] presented an approach for stochastic model updating with covariance matrix adjustment from uncertain experimental modal data. Further, researchers have investigated different problems using stochastic model updating [52,53,61–63]. The majority of those methods can include and estimate of the global model randomness or uncertainties that are assumed to be spatially homogeneous along the structure. By considering that structure parameter values can be spatially distributed in nature, Adhikari and Friswell [64] estimated distributed parameters modelled as realizations of a random field using modal parameters.

The main goal of this paper is to investigate the use of sensitivity-based model updating with measured FRFs to estimate spatially distributed parameters. The distributed parameters are assumed to be realizations of a random process, which is more realistic for simulating the variability caused by the manufacturing process. The study uses a beam structure where the uncertainty is included in the flexural bending and mass per unit of length modelled by SEM. Such distributed deviations are unknown *a priori* and therefore can be considered to be samples from a random field, which is discretized into random variables using the KL expansion. The implemented technique is validated in a numerical simulation and then applied to experimental data for a polymer beam manufactured by 3D printing.

2. Spectral element method for stochastic systems

By supposing a linear damped distributed parameter dynamic system governed by a linear differential equation [65]

$$\rho_0 \frac{\partial^2 \mathbf{U}(\mathbf{r},t)}{\partial t^2} + L_{10}\frac{\partial \mathbf{U}(\mathbf{r},t)}{\partial t} + L_{20}\mathbf{U}(\mathbf{r},t) = 0 \tag{1}$$

where $\mathbf{U}(\mathbf{r},t)$ is the time dependent displacement variable, $\mathbf{r} \in \mathbb{R}$ is the spatial position vector, and t is time specified in some domain $\mathcal{D}$. In the frequency domain we can write Eq. (1) as:

$$-\omega^2 \rho_0 \mathbf{u}(\mathbf{r},\omega) + i\omega L_{10}\{\mathbf{u}(\mathbf{r},\omega)\} + L_{20}\{\mathbf{u}(\mathbf{r},\omega)\} = 0 \tag{2}$$

Similar to FEM, the frequency-dependent displacement within an element can be interpolated from the nodal displacements $u_e(\mathbf{r},\omega) = \mathbf{g}(\mathbf{r},\omega)^T \hat{\mathbf{u}}_e(\omega)$, where $\hat{\mathbf{u}}_e(\omega)$ is the nodal displacement vector and $\mathbf{g}(\mathbf{r},\omega)$ is the vector of frequency-dependent shape functions represented by

$$\mathbf{g}(\mathbf{r},\omega) = \mathbf{\Gamma}(\omega)\mathbf{s}(\mathbf{r},\omega) \tag{3}$$

where $\mathbf{\Gamma}(\omega)$ is a complex matrix that depends on the boundary conditions and $\mathbf{s}(\mathbf{r},\omega)$ is a vector containing exponential functions $[e^{-ik(\omega)x}]$. One of the advantages using SEM is that only one element is required for a homogeneous structural member. The global dynamic spectral matrix for a undamped deterministic system can be described as

$$D_0(\omega) = -\omega^2 \mathbf{M}(\omega) + \mathbf{K}(\omega) \tag{4}$$

In a weak form, frequency-dependent $n \times n$ complex stiffness and mass matrices can be expressed as

$$K(\omega) = \int_{\mathcal{D}} k_s(\mathbf{r}) L_{20}\{\mathbf{g}(\mathbf{r},\omega)\} L_{20}\{\mathbf{g}(\mathbf{r},\omega)\}^T dr \tag{5}$$

and

$$M(\omega) = \int_{\mathcal{D}} \rho(\mathbf{r})\mathbf{g}(r,\omega)\mathbf{g}(r,\omega)^T dr \tag{6}$$

In this present work a spectral element for a straight homogeneous beam is used [6,7,5] and expanded for a stochastic treatment.

2.1. Spectral beam element

The fundamental equations for the flexural motion of a beam structure are briefly described. A more extensive formulation can be found in [6,7]. Fig. 1 shows an elastic two-node beam element with an uniform rectangular cross-section subjected to dynamic forces at both ends. In this section all parameters are assumed to be deterministic variables.

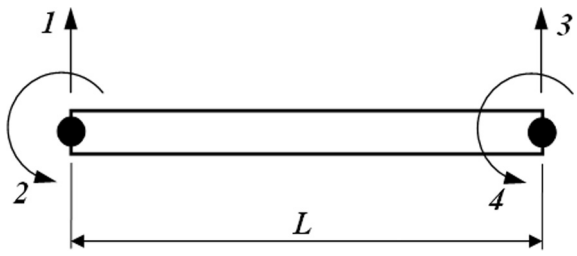

Fig. 1. Two-node beam spectral element.

The equation of motion of a damped Euler-Bernoulli beam under bending vibration may be written as [5],

$$\frac{\partial^2}{\partial x^2}\left[EI(x)\frac{\partial^2 v(x,t)}{\partial x^2}\right]+\rho A(x)\frac{\partial^2 v(x,t)}{\partial t^2}=0 \tag{7}$$

where EI is the bending stiffness, ρA is the mass per unit length, $v(x,t)$ is the transverse flexural displacement, E is the Young's modulus, A is the cross-section area, ρ is the mass density, and I is the inertia moment. A hysteretic structural damping is assumed and introduced into the model formulation by adding an imaginary part proportional to the loss factor η to the Young's modulus. In the deterministic case a complex value given $E=E_0(1+i\eta)$, where E_0 is the Young's modulus mean value, η is the loss factor and $i=\sqrt{-1}$ [6]. In the stochastic case, the complex random variable $E(\theta)$ will follow the complex random variable rules [21]. It is given by $E(\theta)=\widehat{E}(\theta)+E_0 i\eta$, where the random part of the Young's modulus is a real value, $\widehat{E}(\theta)$, and the imaginary part is taken as deterministic $E_0 i\eta$.

By considering the homogeneous differential equation with constant properties along the beam length, the spectral form becomes:

$$\frac{d^4\hat{v}}{dx^4}-\beta^4\hat{v}=0 \tag{8}$$

Eq. (8) can be split into a product of two terms which must vanish. A solution of the type $v(x)e^{i\omega t}=e^{kx}e^{i\omega t}$, where k (wavenumber) is given by:

$$k^4-\beta^4=0 \quad \Rightarrow \quad k=\pm i\beta \text{ or } \pm\beta \tag{9}$$

for

$$\beta^4=\frac{\rho A\omega^2}{EI} \tag{10}$$

where ω is the circular frequency. For the spectral Euler-Bernoulli beam element of length L, the general solution of $v(x)e^{i\omega t}=e^{kx}e^{i\omega t}$ can be then obtained in the form of

$$v(\mathbf{x},\omega)=a_1e^{-ikx}+a_2e^{-kx}+a_3e^{-ik(L-x)}+a_4e^{-k(L-x)}=\mathbf{s}(x,\omega)\mathbf{a} \tag{11}$$

where

$$\begin{aligned}\mathbf{s}(x,\omega)&=\left[e^{-ikx},e^{-kx},e^{-ik(L-x)},e^{-k(L-x)}\right]\\ \mathbf{a}(x,\omega)&=\{a_1,a_2,a_3,a_4\}^T\end{aligned} \tag{12}$$

The spectral nodal displacements and slopes of the beam element

$$\mathbf{d}=\begin{bmatrix}v_1\\ \Theta_1\\ v_2\\ \Theta_2\end{bmatrix}=\begin{bmatrix}v(0)\\ v'(0)\\ v(L)\\ v'(L)\end{bmatrix} \tag{13}$$

can be related to the displacement field at the two nodes ($x=0$ and $x=L$),X by

$$\mathbf{d}=\begin{bmatrix}s(0,\omega)\\ s'(0,\omega)\\ s(L,\omega)\\ s'(L,\omega)\end{bmatrix}\mathbf{a}=\mathbf{\Gamma}(\omega)\mathbf{a} \tag{14}$$

where

$$\mathbf{\Gamma}(\omega)=\begin{bmatrix}1 & 1 & e^{-ikL} & e^{-kL}\\ -ik & -k & ie^{-ikL}k & e^{-kL}k\\ e^{-ikL} & e^{-kL} & 1 & 1\\ -ie^{-ikL}k & -e^{-kL}k & ik & k\end{bmatrix} \tag{15}$$

The frequency-dependent displacement within an element is interpolated from the nodal displacement vector $\mathbf{d}$ by eliminating the constant vector $\mathbf{a}$ from Eq. (13) and using Eq. (14) it can be expressed as

$$v(x,\omega)=\mathbf{g}(x,\omega)\mathbf{d} \tag{16}$$

where the shape function can be expressed as

$$\mathbf{g}(\mathbf{x},\omega)=\mathbf{s}(\mathbf{x},\omega)\boldsymbol{\Gamma}^{-1}(\omega)=\left\{\begin{matrix} g_1(x)\\ g_2(x)\\ g_3(x)\\ g_4(x)\end{matrix}\right\}^T \tag{17}$$

$$=\left\{\begin{matrix} \dfrac{-2\cos(kx)-2\cosh(kx)+(1-i)(\cos(k((1+i)L-x))+i\cos(k((1+i)L-ix))+\cosh(k((1+i)L-x))+i\cosh(k((1+i)L-ix)))}{4\cos(kL)\cosh(kL)}\\ -\dfrac{2\sin(kx)+2\sinh(kx)+(1+i)(\sin(k((1+i)L-x))-\sin(k((1+i)L-ix))+\sinh(k((1+i)L-x))-\sinh(k((1+i)L-ix)))}{4k(\cos(kL)\cosh(kL)-1)}\\ \dfrac{\cos(k(L-x))-\cos(kx)\cosh(kL)+\cosh(k(L-x))-\cos(kL)\cosh(kx)+\sin(kx)\sinh(kL)-\sin(kL)\sinh(kx)}{2-2\cos(kL)\cosh(kL)}\\ \dfrac{\sin(k(L-x))-\cos(kx)\sinh(kL)+\cosh(kx)(\sinh(kL)-\sin(kL))+\cosh(kL)(\sin(kx)-\sinh(kx))+\cos(kL)\sinh(kx)}{2k(\cos(kL)\cosh(kL)-1)}\end{matrix}\right\}^T$$

In the case of the Euler-Bernoulli beam, a generalized transverse displacement at an arbitrary point can be expressed as (Eq. (16)),

$$v(x)=g_1(x)v_1+g_2(x)\Theta_1+g_3(x)v_2+g_4(x)\Theta_2$$

The damping is assumed hysteric and for this reason only the (4×4) mass and (4×4) stiffness matrices will be determined in a weak form:

$$\mathbf{K}_0(\omega)=\int_0^L EI_0(x)\mathbf{g}''(x)\mathbf{g}''^T(x)dx \tag{18}$$

and

$$\mathbf{M}_0(\omega)=\int_0^L \rho A_0(x)\mathbf{g}(x)\mathbf{g}^T(x)dx \tag{19}$$

where $'$ express the spatial partial derivative. The stochastic beam spectral element is formulated as a random process expanded in a spectral KL decomposition.

2.2. Karhunen-Loève expansion

Since the equations of motion for the beam spectral element are written as partial differential equations, it would be very difficult to apply random fields directly to them. To overcome this difficulty the random field is discretized in terms of random variables. By doing this, many mathematical procedures can be used to solve the resulting discrete stochastic differential equations. The procedure applied here is a random field spectral decomposition using the KL expansion. Assuming that the spectral covariance function is finite, symmetric and positive definite, it can be represented by a spectral decomposition, similar to a Fourier series expansion. By using this concept a random field can be expressed as a generalized Fourier series,

$$\varpi(\mathbf{r},\theta)=\varpi_0(\mathbf{r})+\sum_{j=1}^{\infty}\xi_j(\theta)\sqrt{\lambda_j}\varphi_j(\mathbf{r}) \tag{20}$$

where $\varpi(\mathbf{r},\theta)$ is a random field with covariance function $C_{\varpi}(\mathbf{r}_1,\mathbf{r}_2)$, θ denotes an element of the sample space Ω, so that $\theta\in\Omega$, and $\xi_j(\theta)$ are uncorrelated random variables. The subscript 0, in $\varpi_0(\mathbf{r})$ implies the corresponding deterministic part. The constants λ_j and functions $\varphi_j(\mathbf{r})$ are, respectively, eigenvalues and eigenfunctions satisfying the integral equation:

$$\int_D C_{\varpi}(\mathbf{r}_1,\mathbf{r}_2)\varphi_j(\mathbf{r}_1)d\mathbf{r}_1=\lambda_j\varphi_j(\mathbf{r}_2)\quad \forall j=1,2,\ldots. \tag{21}$$

In this paper one dimensional spaces are considered. Since a Gaussian random field is representative of many physical systems and closed form expressions for the KL expansion exist, a Gaussian autocorrelation function with exponential decay will be assumed here. It can be expressed as,

$$C(x_1,x_2)=e^{-|x_1-x_2|/\mathtt{b}} \tag{22}$$

where $\mathtt{b}$ is the correlation length, which is an important parameter to describe the random field. A random field can be expanded in a finite basis of deterministic functions and random variables if the correlation length is large compared with the domain under consideration; for more details, see [3]. An analytical solution in the interval $-\mathtt{a}<x<\mathtt{a}$ where it is assumed that the mean is zero, produces a random field as,

$$\varpi_1(x,\theta)=\sum_{j=1}^{\infty}\xi_j(\theta)\sqrt{\lambda_j}\varphi_j(x) \tag{23}$$

Defining $\mathtt{c}=1/\mathtt{b}$, the corresponding eigenvalues and eigenfunctions for odd j are given by [3],

$$\lambda_j = \frac{2\mathtt{c}}{\omega_j^2 + \mathtt{c}^2}; \quad \varphi_j(x) = \frac{\cos\left(\omega_j \frac{L}{2}\right)}{\sqrt{\mathtt{a} + \frac{\sin(2\omega_j \mathtt{a})}{2\omega_j}}} \qquad \text{where} \quad \tan(\omega_j \mathtt{a}) = \frac{\mathtt{c}}{\omega_j} \tag{24}$$

and for even j are given by,

$$\lambda_j = \frac{2\mathtt{c}}{\omega_j^2 + \mathtt{c}^2}; \quad \varphi_j(x) = \frac{\sin\left(\omega_j \frac{L}{2}\right)}{\sqrt{\mathtt{a} - \frac{\sin(2\omega_j \mathtt{a})}{2\omega_j}}} \qquad \text{where} \quad \tan(\omega_j \mathtt{a}) = \frac{\omega_j}{-\mathtt{c}} \tag{25}$$

These eigenvalues and eigenfunctions will be used to obtain the stochastic dynamic stiffness matrices for beam spectral elements.

For practical applications, Eq. (23) is truncated with M terms, which can be selected based on the amount of information to be kept. Its value is also related with the correlation length and the number of eigenvalues kept, provided that they are arranged in decreasing order.

2.3. Stochastic beam spectral element

In this work the flexural bending ($EI(x)$) and mass per unit length ($\rho A(x)$) are considered as spatially distributed random variables. Therefore, the flexural bending is assumed as a random field of the form:

$$EI(x,\theta) = EI_0[1 + \varepsilon_1 \varpi_1(x,\theta)] \tag{26}$$

and the mass per unit of length is assumed a random field as

$$\rho A(x,\theta) = \rho A_0[1 + \varepsilon_2 \varpi_2(x,\theta)] \tag{27}$$

The subscript 0 indicates the mean value, $0 < \varepsilon_i \ll 1 (i = 1, 2, \ldots)$ are deterministic constants and the random field $\varpi_i(x,\theta)$ is taken to have zero mean, unit standard deviation and covariance $R_{ij}(\xi)$. Since, $EI(x,\theta)$ and $\rho A(x,\theta)$ are strictly positive, $\varpi_i(x,\theta)(i = 1, 2, \ldots)$ is rigorously required to satisfy the probability condition $\mathrm{P}[1 + \varepsilon_i \varpi_i(x,\theta) \leqslant 0] = 0$. This requirement would exclude the use of Gaussian models for these random fields. However, for small ε_i, it is expected that Gaussian models can still be used if the primary interest of the analysis is to estimate the first few response moments and not the response behaviour near tails of the probability distributions. Expanding the random fields $\varpi_1(x,\theta)$ and $\varpi_2(x,\theta)$ in a KL spectral decomposition one obtains the (4×4) stochastic dynamic stiffness matrix written as,

$$\begin{aligned} \mathbf{D}(\omega,\theta) &= \mathbf{D}_0(\omega) + \Delta\mathbf{D}(\omega,\theta) \\ &= -\omega^2[\mathbf{M}_0(\omega) + \Delta\mathbf{M}(\omega,\theta)] + [\mathbf{K}_0(\omega) + \Delta\mathbf{K}(\omega,\theta)] \end{aligned} \tag{28}$$

where the deterministic part is given by Eqs. (18) and (19), and the random part $\Delta\mathbf{D}(\omega,\theta)$ is related to the stiffness and mass coefficients $\Delta\mathbf{K}(\omega,\theta)$ and $\Delta\mathbf{M}(\omega,\theta)$, respectively, expanded in a KL decomposition of the form

$$\Delta\mathbf{K}(\omega,\theta) = \varepsilon_1 \sum_{j=1}^{N_K} \xi_{Kj}(\theta) \sqrt{\lambda_{Kj}} \mathbf{K}_j(\omega) \tag{29}$$

and

$$\Delta\mathbf{M}(\omega,\theta) = \varepsilon_2 \sum_{j=1}^{N_M} \xi_{Mj}(\theta) \sqrt{\lambda_{Mj}} \mathbf{M}_j(\omega) \tag{30}$$

where N_k and N_M are the numbers of terms kept in the KL expansion; $\xi_{Kj}(\theta)$ and $\xi_{Mj}(\theta)$ are uncorrelated Gaussian random variables with zero mean and unit standard deviation. The constant (4×4) matrices $\mathbf{K}_j(\omega)$ and $\mathbf{M}_j(\omega)$ can be expressed as

$$\mathbf{K}_j(\omega) = EI_0 \int_0^L \varphi_{Kj}(x_e + x) \mathbf{g}''(x) \mathbf{g}''^T(x) dx \tag{31}$$

$$\mathbf{M}_j(\omega) = \rho A_0 \int_0^L \varphi_{Kj}(x_e + x) \mathbf{g}(x) \mathbf{g}^T(x) dx \tag{32}$$

where x_e the local coordinate. Substituting Eqs. (24) and (25) in Eqs. (31) and (32), the closed-form expressions for the random part of the stiffness and mass matrices for the beam spectral element in odd j can be expressed as

$$\mathbf{K}_j(\omega) = \frac{EI_0}{\sqrt{\mathtt{a} + \frac{\sin(2\omega_j \mathtt{a})}{2\omega_j}}} \left[\int_0^L \cos(\omega_j (x_e + x)) \mathbf{g}''(x) \mathbf{g}''^T(x) dx \right] \tag{33}$$

$$\mathbf{M}_j(\omega) = \frac{\rho A_0}{\sqrt{\mathtt{a} + \frac{\sin(2\omega_j \mathtt{a})}{2\omega_j}}} \left[\int_0^L \cos(\omega_j(x_e + x)) \mathbf{g}(x) \mathbf{g}^T(x) dx \right] \tag{34}$$

and for even j it is given by

$$\mathbf{K}_j(\omega) = \frac{EI_0}{\sqrt{\mathtt{a} - \frac{\sin(2\omega_j \mathtt{a})}{2\omega_j}}} \left[\int_0^L \sin(\omega_j(x_e + x)) \mathbf{g}''(x) \mathbf{g}''^T(x) dx \right] \tag{35}$$

$$\mathbf{M}_j(\omega) = \frac{\rho A_0}{\sqrt{\mathtt{a} - \frac{\sin(2\omega_j \mathtt{a})}{2\omega_j}}} \left[\int_0^L \sin(\omega_j(x_e + x)) \mathbf{g}(x) \mathbf{g}^T(x) dx \right] \tag{36}$$

3. Sensitivity-based updating method using FRFs

The objective of sensitivity based parameter estimation methods is to improve the correlation between the measured and predicted responses. The correlation is determined by an objective function involving modal or dynamic response data. In general, they are non-linear functions with respect to the model parameters, and so an iterative procedure is required with the possible associated convergence problems [27]. The non-linear least squares method uses a truncated Taylor series expansion of the dynamic response in terms of the unknown parameters, often limited to the first two series terms, yielding the linear approximation:

$$\delta \mathbf{H} = \mathbf{S}_j \delta \boldsymbol{\xi}, \tag{37}$$

where $\delta \mathbf{H} = \mathbf{H}_m - \mathbf{H}_j$ is the residual of the measured output, $\delta \boldsymbol{\xi} = \boldsymbol{\xi} - \boldsymbol{\xi}_j$ is the perturbation in the parameters, and $\mathbf{S}_j$ is the sensitivity matrix. It contains the derivatives of the frequency response functions with respect to the chosen parameters to be varied, ξ_j. The iteration is initialized with ξ_0 equal to 0 and it is assumed that there are more measured data than unknown parameters. Then, Eq. (37) provides an over-determined set of simultaneous equations that can be solved using a least squares solution. Adopting the weighted objective function:

$$J(\delta \xi) = \varepsilon^T \mathbf{W}_e \varepsilon, \tag{38}$$

where $\varepsilon = \delta \mathbf{H} - \mathbf{S}_j \delta \boldsymbol{\xi}$ is the error in the predicted measurements based on the updated parameters and $\mathbf{W}_e$ is a positive definite weighting matrix. Substituting ε in Eq. (38) leads to

$$J(\delta \xi) = \mathbf{W}_e \delta \mathbf{H} \delta \mathbf{H}^T - \mathbf{W}_e (\mathbf{S}_j \delta \mathbf{H}^T \delta \boldsymbol{\xi} + \mathbf{S}_j^T \delta \mathbf{H} \delta \boldsymbol{\xi}^T) + \delta \boldsymbol{\xi} \mathbf{S}_j \mathbf{W}_e \mathbf{S}_j^T \delta \boldsymbol{\xi}^T. \tag{39}$$

Minimizing J with respect to $\delta \boldsymbol{\xi}$ is equivalent to:

$$\nabla J(\delta \xi) = 0 = -\mathbf{S}_j \mathbf{W}_e \delta \mathbf{H}^T + \mathbf{S}_j \mathbf{S}_j^T \mathbf{W}_e \delta \boldsymbol{\xi}, \tag{40}$$

and solving Eq. (40) for $\delta \boldsymbol{\xi}$ results,

$$\delta \xi = [\mathbf{S}_j^T \mathbf{W}_e \mathbf{S}_j]^{-1} \mathbf{S}_j^T \mathbf{W}_e \delta \mathbf{H}. \tag{41}$$

Thus, the updated parameter can be obtained from:

$$\boldsymbol{\xi}_{j+1} = \boldsymbol{\xi}_j + [\mathbf{S}_j^T \mathbf{W}_e \mathbf{S}_j]^{-1} \mathbf{S}_j^T \mathbf{W}_e (\mathbf{H}_m - \mathbf{H}_j). \tag{42}$$

The solution of Eq. (42) can be ill-conditioned, which might be a central problem in this kind of method. The treatment of ill-conditioning is explained in [66–69,32]. Titurus and Friswell [70] presented a regularization treatment within the context of sensitivity-based FE model updating, which is used in this paper. The method gives the updated parameter vector as:

$$\boldsymbol{\xi}_{j+1} = \boldsymbol{\xi}_j + [\mathbf{S}_j^T \mathbf{W}_e \mathbf{S}_j + \gamma^2 \mathbf{W}_p]^{-1} \{\mathbf{S}_j^T \mathbf{W}_e (\mathbf{H}_m - \mathbf{H}_j)\}. \tag{43}$$

The regularization parameter $\gamma \in [01]$ determines the relative weight between the regularized solution ($\|\boldsymbol{\xi}_{j+1} - \boldsymbol{\xi}_j\|$) versus the corresponding residual norm ($\|\S_j(\boldsymbol{\xi}_{j+1} - \boldsymbol{\xi}_j) - (\mathbf{H}_m - \mathbf{H}_j)\|$). The size of the regularisation parameter γ will provides the balance between the residual ($\|\mathbf{H}_m - \mathbf{H}_j\|$) and the parameter change ($\boldsymbol{\xi}_{j+1} - \boldsymbol{\xi}_j$). For γ too small the problem will be too close to the original ill-posed problem, while γ too large the problem solved will have little connection with the original problem [67]. Link [71] suggested the regularisation parameter γ^2 lies between 0 and 0.3. Accordingly, in this paper the regularization parameter was assumed as 0.3. The updated parameter is evaluated in an iterative process until convergence, which is determined when the change in parameters, $\|\boldsymbol{\xi}_{j+1} - \boldsymbol{\xi}_j\|$ or the FRF $\|\mathbf{H}_m - \mathbf{H}_j\|$ is sufficiently small.

The choice of the weighting matrices is a difficult subject, and estimated statistical properties can be employed [27]. Here, we use a solution procedure presented by Grafe [47] where no explicit statistical calculations of the weighting factors are required and the correlation coefficient $(X_s(\omega))$ is used directly as

$$[diag(\mathbf{W_e})] = [diag(X_s(\omega))] \tag{44}$$

The correlation coefficient is based on the Modal Assurance Criterion (MAC) theory [72,73]. For any measured frequency the correlation coefficient is a correlation between the measured and predicted response vectors, given by

$$X_s(\omega) = \frac{\left|\{H_m(\omega)\}^H\{H_a(\omega)\}\right|^2}{(\{H_m(\omega)\}^H\{H_m(\omega)\})(\{H_a(\omega)\}^H\{H_a(\omega)\})} \tag{45}$$

where $H_m(\omega)$ and $H_a(\omega)$ are the measured and predicted FRF vectors at matching excitation/response locations, respectively. $X_s(\omega)$ assumes a value between zero ($X_s(\omega) = 0$) that indicates no correlation exists and unity ($X_s(\omega) = 1$) which signifies perfect correlation. The correlation coefficient is sensitive to discrepancies in the global deflection shape of the structure. However analogous to the MAC, it is unable to detect scaling errors. A definition of parameter weighing matrix ($\mathbf{W}_p$) was proposed by Link [74] and later by Mottershead and Foster [69]. Similar to the approach of Link[74], the parameter weighing matrix used here is expressed as

$$[\backslash\mathbf{W}_{p\backslash}] = \frac{\|[w_e]\|_2}{max(diag([w_e]))}[\backslash diag([w_e])_\backslash] \tag{46}$$

where $[w_e] = [[\mathbf{S}][\backslash\mathbf{W}_{e\backslash}][\mathbf{S}]^T]^{-1}$.

3.1. Stochastic sensitivity of the FRF

The sensitivity method is based on the linearisation of the non-linear relationship between measurable outputs (modal data or frequency response functions) and the model parameters to be estimated [32]. By considering that in practice the measured raw data obtained from the experimental test are the FRF, in this paper the sensitivity of the FRF will be used. The coefficients of the KL expansion are assumed as uncertain parameters and will be estimated by Eq. (42). By following [40,42,46,47] the deterministic FRF sensitivity related to a general parameter φ can be written as:

$$\frac{\partial\mathbf{H}(\omega)}{\partial\varphi} = -\mathbf{H}(\omega)\frac{\partial\mathbf{D}(\omega)}{\partial\varphi}\mathbf{H}(\omega) \tag{47}$$

where $\mathbf{H}(\omega) = \mathbf{D}^{-1}(\omega)$ is the inverse of the deterministic dynamic stiffness matrix. In the stochastic context, two techniques can be applied. The fist one estimates a random variable, $\varphi(\theta)$. The second one is associated with the parameter ξ_{Kj} of the KL expansion, which are the uncorrelated random variables of the random field. With the first approach Eq. (47) becomes:

$$\frac{\partial\mathbf{H}(\omega,\theta)}{\partial\varphi(\theta)} = -\mathbf{H}(\omega,\theta)\frac{\partial\mathbf{D}(\omega,\theta)}{\partial\varphi(\theta)}\mathbf{H}(\omega,\theta) \tag{48}$$

where $\mathbf{H}(\omega,\theta) = \mathbf{D}^{-1}(\omega,\theta)$, which is inverse of the stochastic dynamic stiffness matrix (Eq. (28)). In the second approach, used in this paper, Eq. (47) is described by:

$$\frac{\partial\mathbf{H}(\omega,\theta)}{\partial\boldsymbol{\xi}} = -\mathbf{H}(\omega,\theta)\left[\frac{\partial\mathbf{K}(\omega,\theta)}{\partial\xi_{Kj}} - \omega^2\frac{\partial\mathbf{M}(\omega,\theta)}{\partial\xi_{Mj}}\right]\mathbf{H}(\omega,\theta) \tag{49}$$

the derivative of $\mathbf{K}(\omega,\theta)$ and $\mathbf{M}(\omega,\theta)$ related to the parameter ξ_{Kj} produces:

$$\frac{\partial\mathbf{K}(\omega,\theta)}{\partial\xi_{Kj}(\theta)} = \varepsilon_1\sqrt{\lambda_{Kj}}\mathbf{K}_j(\omega) \tag{50}$$

and

$$\frac{\partial\mathbf{M}(\omega,\theta)}{\partial\xi_{Mj}(\theta)} = \varepsilon_2\sqrt{\lambda_{Mj}}\mathbf{M}_j(\omega) \tag{51}$$

Substituting Eqs. (50) and (51) in (49),

$$\frac{\partial\mathbf{H}(\omega,\theta)}{\partial\boldsymbol{\xi}(\theta)} = s_{ij} = -H(\omega)\left[\varepsilon_1\sqrt{\lambda_{Kj}}\mathbf{K}_j(\omega) - \omega^2\varepsilon_2\sqrt{\lambda_{Mj}}\mathbf{M}_j(\omega)\right]H(\omega) \tag{52}$$

In this paper the sensitivities of the receptance FRFs ($\mathbf{H}(\omega,\theta)$) were taken in dB scale [75] with 1 m/N reference. It can be shown that [75]

$$\frac{\partial(20log_{10})|\mathbf{H}(\omega,\theta)|}{\partial\boldsymbol{\xi}(\theta)} \approx 8.6859\left(\frac{\Re(\mathbf{H}(\omega,\theta))\frac{\partial(\mathbf{H}(\omega,\theta))}{\partial\xi(\theta)} + \Im(\mathbf{H}(\omega,\theta))\frac{\partial(\mathbf{H}(\omega,\theta))}{\partial\xi(\theta)}}{\Re(\mathbf{H}(\omega,\theta))^2 + \Im(\mathbf{H}(\omega,\theta))^2}\right) \tag{53}$$

The elements of the sensitivity matrix s_{ij} are given by Eq. (53) and the $N_K + N_M$ dimensional vector of updating parameters ξ is

$$\boldsymbol{\xi} = [\xi_{K_1}, \xi_{K_2} \ldots, \xi_{K_{N_K}} \quad \xi_{M_1}, \xi_{M_2} \ldots, \xi_{M_{N_M}}]^T \tag{54}$$

The elements of the vector $\boldsymbol{\xi}$ are sampled from independent and identically distributed standard Gaussian random variables (i.e., with zero-mean and unit standard deviation) from the KL expansion. The parameter vector $\boldsymbol{\xi}$ will be estimated from the measured FRF and used to reconstruct the $EI(x,\theta)$ and $\rho A(x,\theta)$ random field realizations. Once the parameters ξ are obtained, the estimated FRF can be calculated as $\mathbf{H}(\boldsymbol{\xi})$.

4. Numerical and experimental tests

The objective is to show the efficiency of the developed technique. A free-free beam structure is considered and modelled by a two-node beam spectral element with variabilities considered for the beam flexural rigidity EI and for the mass per unit of length ρA. The measured FRF simulates the receptance FRF with an impact force excitation at node 1 and displacement response measured at some points along the beam. The nominal physical properties and geometrical parameters of the beam are: $L = 0.33$ m, $h = 0.006$ m, $b = 0.018$ m, $\eta = 0.1, E = 1.198$ GPa, and $\rho = 1140$ kg/m^3. It is assumed that a variation of the value of EI and ρA can be modelled by a homogeneous Gaussian random field. For the numerical calculations we considered $\epsilon_1 = \epsilon_2$ = 20% of variation with a correlation length of $\mathfrak{b} = L/3$.

4.1. Numerical cases

Two initial cases were carried out with noise-free simulated FRFs which are referred to as synthetic measured FRF. In the first case, an investigation of how the number of FRFs considered can increase the amount of information and yield more accurate parameter estimates. A random field estimation of the beam flexural rigidity and mass per unit of length was performed. The data was generated using 4 terms in the KL expansion, simulating a physically realistic property. We use the FRFs obtained at beam length positions $(0 * L)$, $(0.25 * L)$, $(0.70 * L)$, and (L) of the perturbed beam element. In this case, the objective is to reconstruct the distributed flexural rigidity (EI) function and mass per unit of length (ρA) from the synthetic measured FRFs obtained with a sample of the stochastic beam model.

The flexural rigidity random field sample estimated with 1, 2, 3 and 4 FRFs, and 4 terms in the KL expansion is shown in Fig. 2. In all cases, the reconstructed functions are close to the simulated functions which generated the synthetic measured data. Analogously, the mass random field sample estimated is shown in Fig. 3. Both reconstructed random field samples using only one FRF showed the least effective estimation. By including FRFs in the updating procedure one can improve the information and a better estimation can be achieved. In this numerical example, two FRFs are suitable for the analysis, given that the estimation using more than two FRFs did not present major improvements. Because of the increased information when more FRFs are included in the updating procedure, better estimation for the reconstructed random field samples were obtained.

The reconstructed random field samples are used to calculate the FRF of the stochastic beam at each iteration in the optimisation procedure. The comparison between the synthetic measured, initial and updated FRF is shown in Figs. 4–7. In all cases of this first test (estimation with 1, 2, 3 and 4 FRFs), the initial FRFs are calculated assuming deterministic homogeneous EI and ρA, in the end of the iteration procedure the FRFs calculated with the estimated parameters is closer to the synthetic measured FRF. The FRFs exhibit a high level of correlation as it can be seen in the correlation coefficients plotted in Fig. 8. The high correlation indicates no errors because of its immunity to scaling, i.e., each predicted frequency point can be scaled to match its measured counterpart. For all cases, similar correlation results were obtained.

The iteration convergence stop criterion was the change in the response, $\|\mathbf{H}_m - \mathbf{H}_j\|$ or change in parameter $\|\boldsymbol{\xi}_{j+1} - \boldsymbol{\xi}_j\|$ below 1% and 0,1% of relative error, respectively. Fig. 9(a-d) shows the convergence of the FRFs and updating parameters estimated using 1, 2, 3, and 4 FRFs.

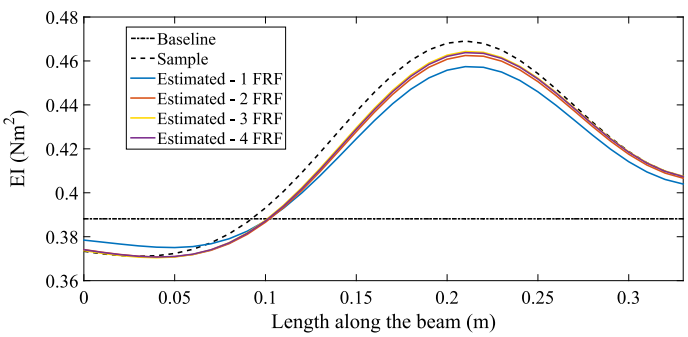

Fig. 2. Baseline, sample and reconstructed random field sample of the flexural rigidity along the length using 1, 2, 3, and 4 FRFs in the estimation.

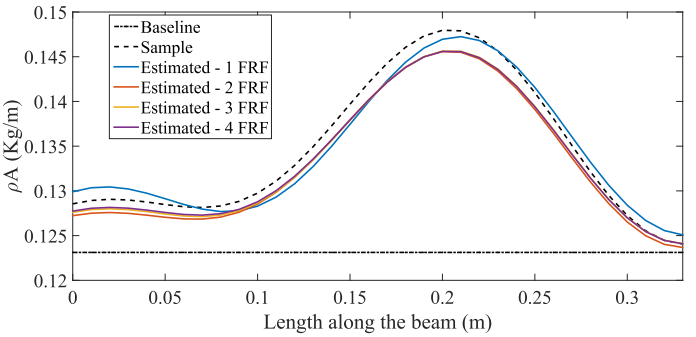

Fig. 3. Baseline, sample and reconstructed random field sample of the mass per unit of length using 1, 2, 3, and 4 FRFs in the estimation.

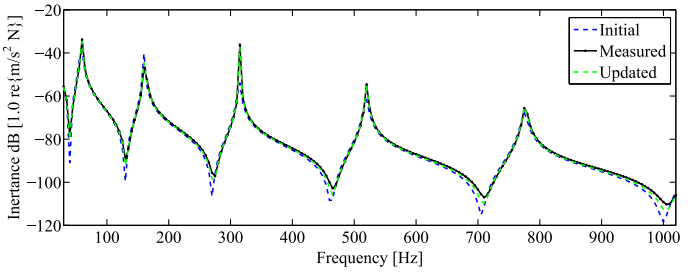

Fig. 4. Comparison between the FRF obtained with an initial value, and updated value, and the synthetic measured FRF using one FRF at node $1(0 * L)$.

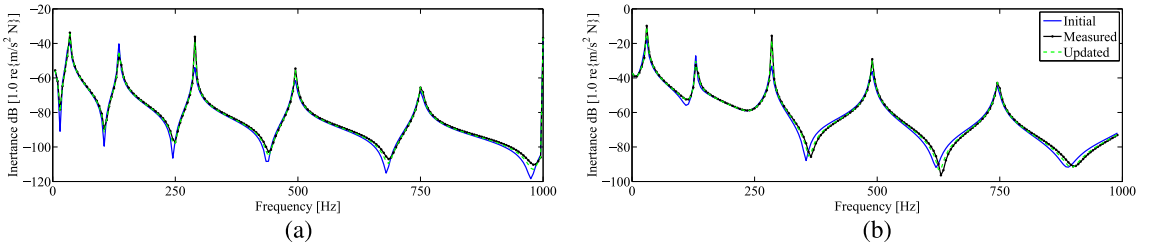

Fig. 5. Comparison between an initial value, updated and the synthetic measured using two FRFs (a) at $0 * L$ and (b) at $0.25 * L$.

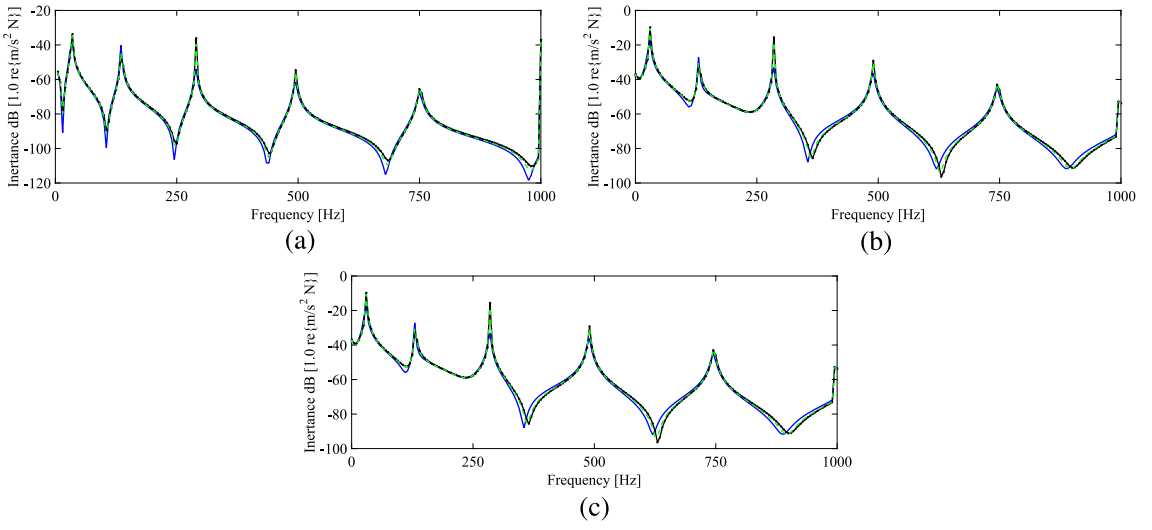

Fig. 6. Comparison between an initial value, updated and the synthetic measured using three FRFs (a) at $0 * L$, (b) at $0.25 * L$, and (c) at $0.70 * L$.

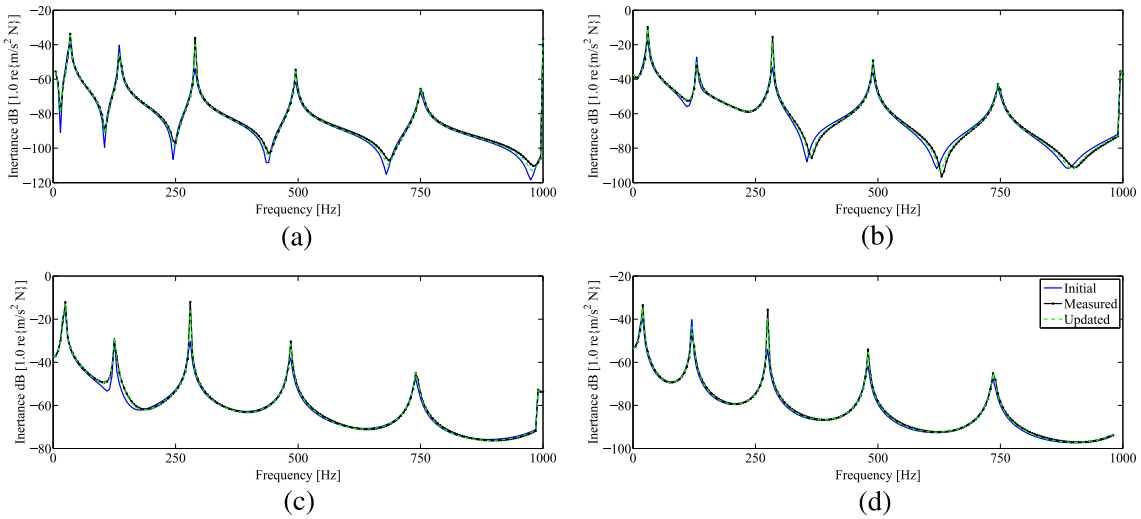

Fig. 7. Comparison between an initial value, updated and the synthetic measured using four FRFs (a) at $0 * L$, (b) $0.25 * L$, (c) $0.70 * L$, and (d) L.

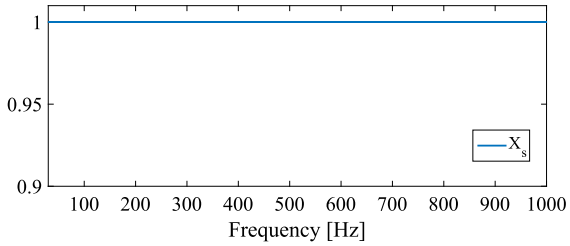

Fig. 8. FRF correlation coefficient $(X_s(\omega))$.

In the second case, it was fixed in two the number of FRFs used in the estimation and varied the number of terms in the KL expansion. The FRFs used were measured at node 1 and 2. Two other samples of random field data were generated with 12 terms in the KL expansion. The estimation of distributed parameters, EI and ρA, was performed with 4, 8 and 12 terms in the expansion, and similar stop criteria was assumed. As in the last test, the objective is to reconstruct the distributed flexural rigidity and mass from the synthetic measured FRFs obtained with a sample of the stochastic model. However, the random field samples are estimated with a different number of terms.

Figs. 10 and 11 show the flexural rigidity and mass random field sample estimations, respectively. As mentioned, the samples were simulated with 12 modes in the KL expansion and the estimation performed using 4 (shown in Fig. 11 on the left had side, 8 (shown in the middle), and 12 (shown in the right hand side) parameters (ξ). Although the terms in the KL expansion cannot be precisely estimated from the data, note that both reconstructed distributed random parameters presented a good approximation of the sample distributed parameters. Obviously, the random field samples reconstructed with the same number as the actual sample can better represent the distributed parameter. However, the reconstruction performed with 4 and 8 modes was reasonable.

Next, the reconstructed flexural rigidity EI and mass per unit of length ρA were used to calculate the frequency response function of the stochastic beam at each iteration of the optimisation procedure. The responses used 4, 8 and 12 terms in KL expansion, are shown in Figs. 12–14, respectively. They show the comparison between initial, synthetic measured, and estimated FRFs. In all cases, the comparison between the updated and synthetic measured FRFs showed a suitable approximation. Fig. 15 shows that the correlation function $(X_s(\omega))$ is unity across the full spectrum. The major part of the corrections was introduced by the first iterations and subsequent iterations introduced only minor adjustments. In Fig. 16 the graphics show the evolution of the iteration process until the change in the FRFs or change in the updating parameters with 4, 8, and 12 terms in KL expansion falls under a determined threshold value. In this case, similar to the first case, the stop criterion was assumed 0.5% for both.

4.2. Experimental results

A beam made of polyamide (PA) with uniform rectangular cross-section was used in the experimental tests. The beam is 18 mm wide, 6 mm thick, with a mass per unit length of approximately 0.02343 kg/m. The average flexural rigidity (EI) was

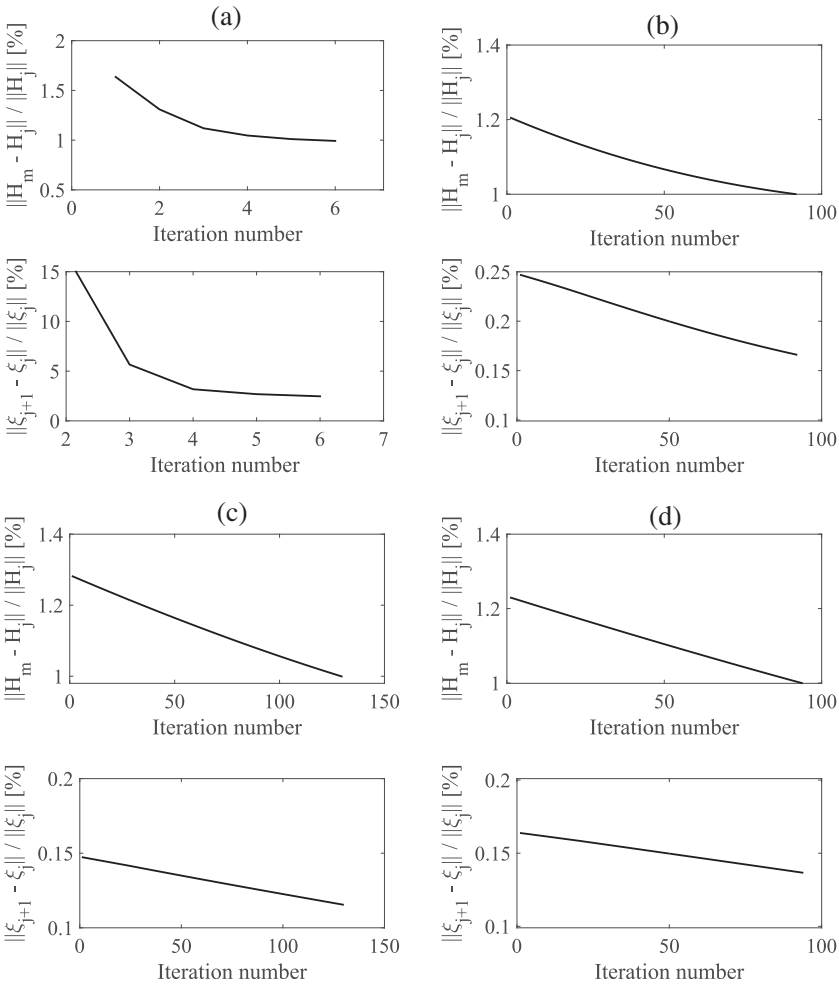

Fig. 9. Convergence of the FRF residual ($\|\mathbf{H}_m - \mathbf{H}_j\|$) and parameters ($\|\boldsymbol{\xi}_{j+1} - \boldsymbol{\xi}_j\|$) using (a) 1 FRF, (b) 2 FRFs, (c) 3 FRFs, and (d) 4 FRFs.

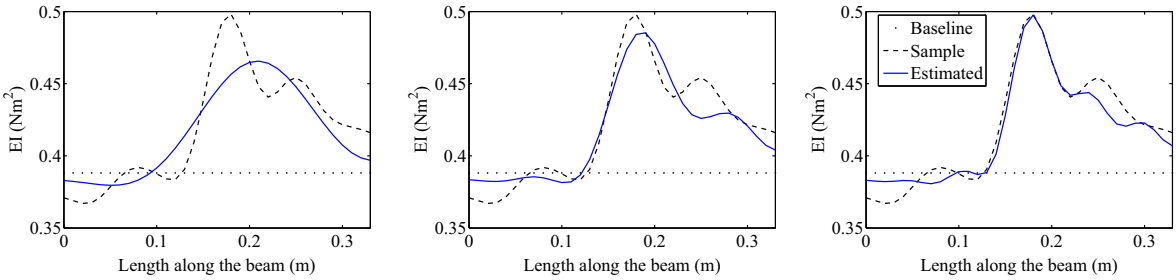

Fig. 10. Baseline, sample and reconstructed random field sample of the flexural rigidity along the length using 4 (LHS), 8 (middle) and 12 (RHS) modes.

obtained experimentally. The beam was manufactured using the Selective Laser Sintering (SLS) technology. As a consequence of the manufacturing process, a variability of the beam properties along its length can be expected. In order to verify the efficiency of the proposed method it was applied to a measured FRF and results were compared with measurements of the flexural rigidity at many points along the beam measured using an ultrasound apparatus. The Young's modulus (E) was measured at 22 points along the beam with an ultrasonic pulse-echo device. The experimental setup is shown in Fig. 17. In this experiment a shear wave transducer (*OlympusU*8403072/*U*8403071) was used. The signals were measured and analysed using an Olympus Parametrics NDT EPOCH 4 Ultrasonic Flaw Detector. The measured Young's modulus E along the beam is

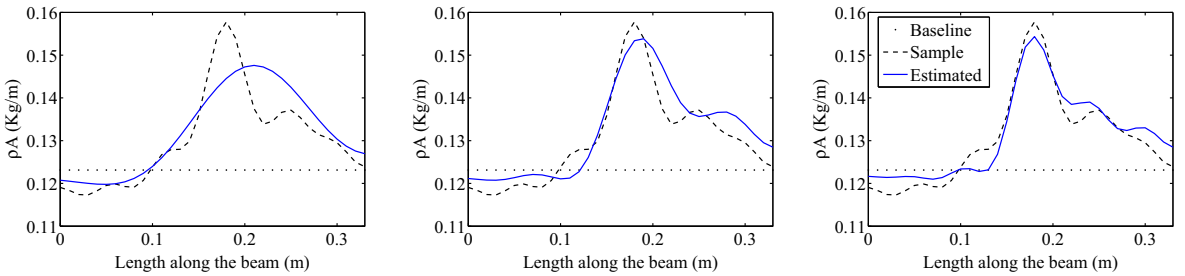

Fig. 11. Baseline, sample and reconstructed random field sample of the mass along the length using 4 (LHS), 8 (middle) and 12 (RHS) modes.

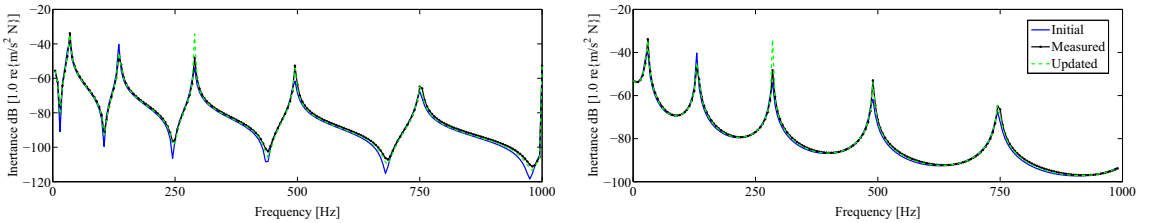

Fig. 12. Comparison among an initial, updated and the synthetic measured FRF at node 1 (LHS) and node 2 (RHS). Updated FRFs calculated with the random field sample reconstructed with 4 modes.

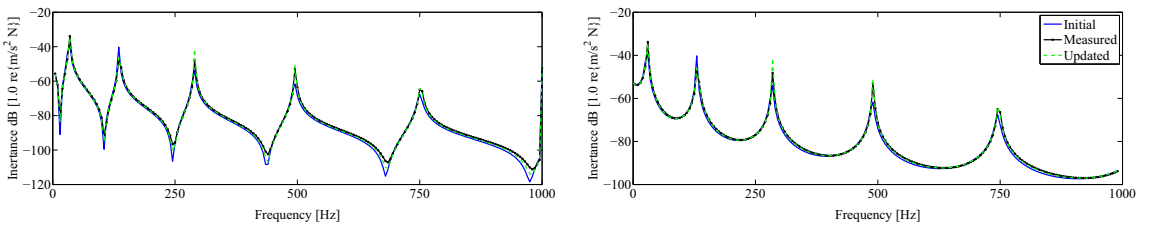

Fig. 13. Comparison among an initial, updated and the synthetic measured FRF at node 1 (LHS) and node 2 (RHS). Updated FRFs calculated with the random field sample reconstructed with 8 modes.

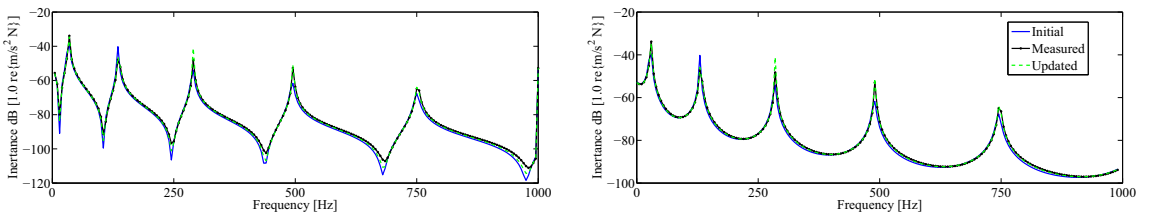

Fig. 14. Comparison among an initial, updated and the measured FRF at node 1 (LHS) and node 2 (RHS). Updated FRFs calculated with the random field sample reconstructed with 12 modes.

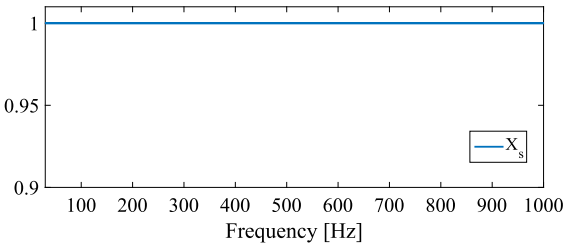

Fig. 15. FRF correlation coefficient ($X_s(\omega)$).

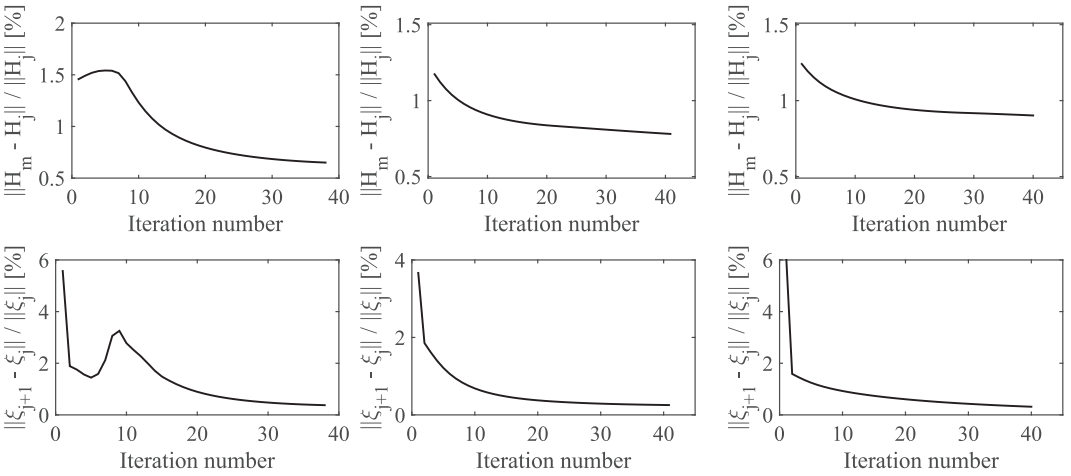

Fig. 16. Convergence of the FRF ($\|\mathbf{H}_m - \mathbf{H}_j\|$) and parameters ($\|\boldsymbol{\xi}_{j+1} - \boldsymbol{\xi}_j\|$) using 4 (LHS), 8 (middle) and 12 (RHS) terms in the KL expansion.

Fig. 17. Procedure for experimental measurement of polyamide beam properties.

shown in Fig. 19, where it is compared with the predicted values using the KL expansion with 4 and 6 estimated parameters. The number of terms in KL expansion was chosen based on the shape sample characteristics.

Fig. 18 shows the second experimental test setup, used to measure the FRFs. The signals were acquired and analysed using LMS Test Lab. The FRFs were estimated with a bandwidth of 1024 Hz and 1024 spectral lines. An impact hammer was used to excite the structure and a micro accelerometer Kistler series 8614A was used to measure the response. The experimental FRFs were obtained by impact force excitation at node 1 and acceleration response at node 1 and node 2. The micro accelerometer mass is considerably small and lightweight compared with the beam so that the accelerometer mass was neglected. To simulate the free-free boundary condition we supported the beam by using a soft polyurethane foam edges.

The initial, measured sample of EI and reconstructed distributed sample with 4 and 6 terms in KL expansion are shown in Fig. 19. The random field experimental sample could not be reconstructed accurately; nevertheless, an acceptable difference between updated and measured FRFs can be observed. Experimental, initial and updated FRFs using 4 and 6 terms in KL expansion are illustrated in Figs. 20 and 21, respectively. Similar stop criteria of the numerical case were applied. Examining both cases, it can be observed that the reconstruction using 6 terms was more appropriated in this test. Even the FRFs updated procedure showed better convergence using 6 terms; However, the reconstructed $EI(x)$ with 4 terms presents a

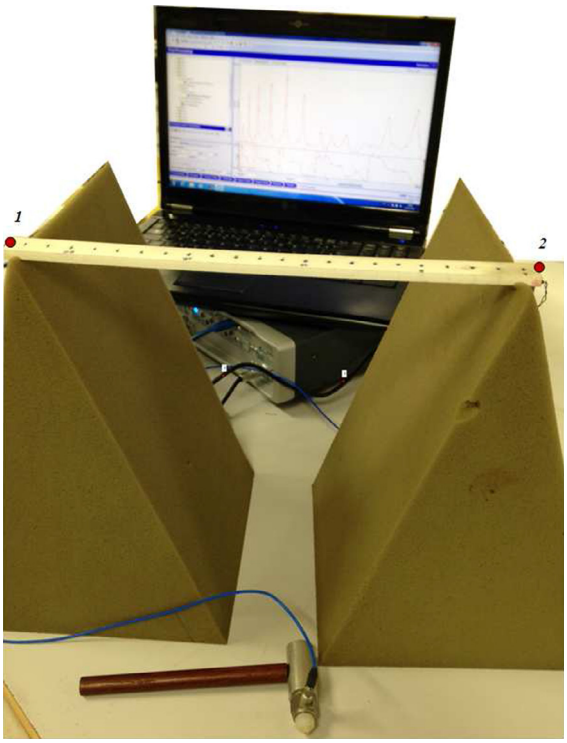

Fig. 18. The test rig for the free-free beam.

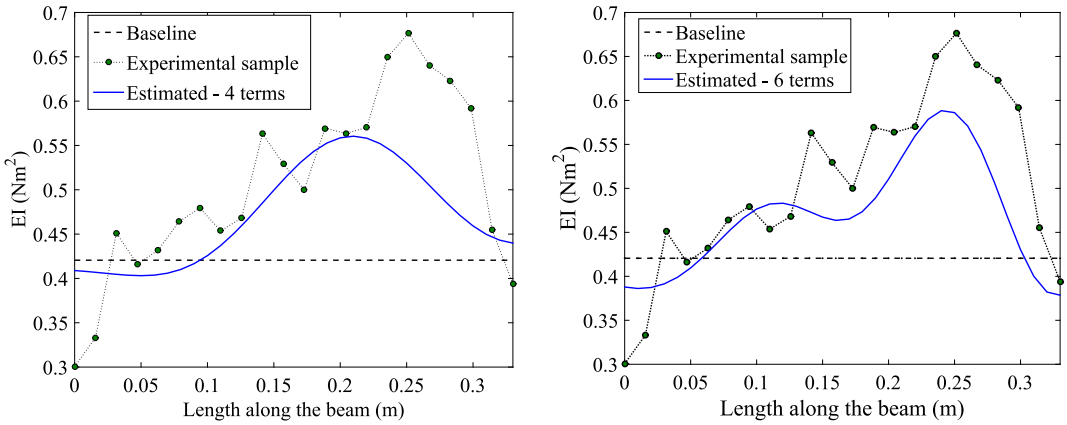

Fig. 19. Baseline, experiential sample and reconstructed random field sample of the flexural rigidity ($EI(x)$) with 4 (LHS) and 6 (RHS) terms in the KL expansion.

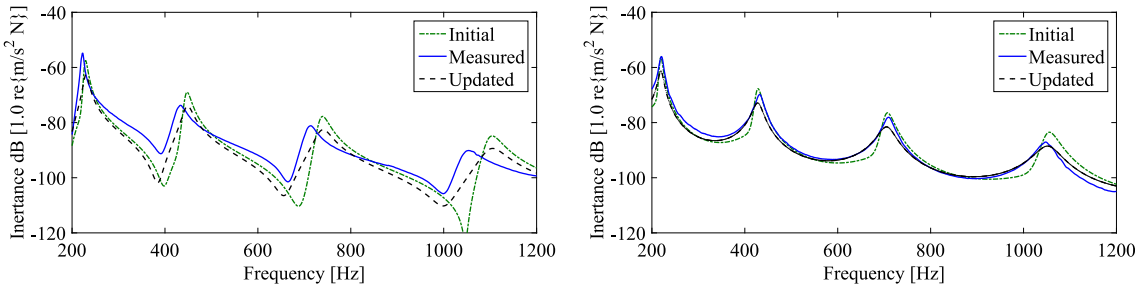

Fig. 20. Comparison between an initial value, updated and the experimental measured FRF at node 1 (LHS) and at node 2 (RHS) using 4 terms in the KL expansion.

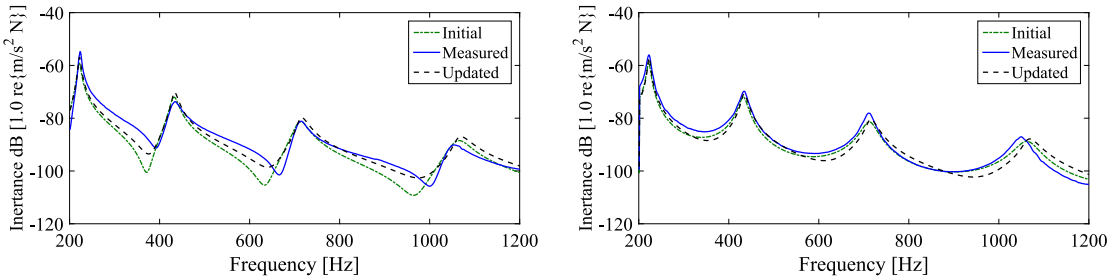

Fig. 21. Comparison between an initial value, updated and the experimental measured FRF at node 1 (LHS) and at node 2 (RHS) using 6 terms in the KL expansion.

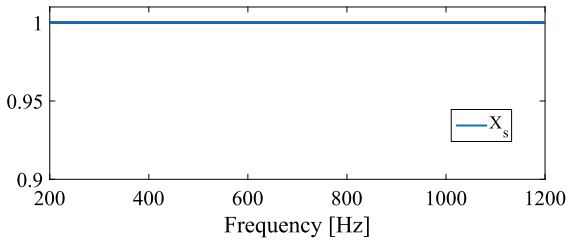

Fig. 22. FRF correlation coefficient ($X_s(\omega)$).

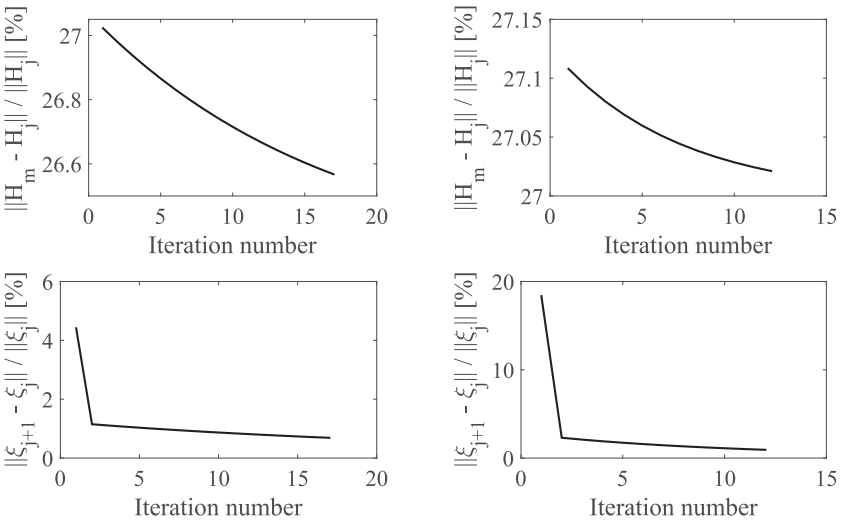

Fig. 23. Convergence of the FRF ($\|\mathbf{H}_m - \mathbf{H}_j\|$) and parameters ($\|\xi_{j+1} - \xi_j\|$) using 4 (LHS) and 6 (RHS) terms in the KL expansion.

good approximation compared with random field sample measured by ultrasound. Fig. 23 shows the iteration process until the change in the FRFs and change in the updating parameters converge with 4, and 6 terms in the KL expansion.

As shown in Fig. 22, the adjustments in the model have led to a high level of correlation. Regarding the numerical and experimental cases presented, it was shown that the proposed method can be used to reconstruct the distributed variability of the beam. In all cases, the random field samples were reconstructed with a certain error associated. In general, all results were satisfactory; close shape of the random field sample was estimated, which demonstrated the performance of the proposed technique. It was also observed that the iteration always stopped after achieving the threshold value for the FRF residual, similarly to the second case.

5. Final remarks

In the present work, a technique to estimate spatially distributed parameters of samples of a stochastic structure using a KL expansion and sensitivity-based FRF model updating was proposed. Randomness was included in the flexural rigidity

(EI) and mass per unit length (ρA) of a beam structure. As a stochastic model is employed, the sensitivity-based method using FRF is also developed for a stochastic model based on a spectral beam element. To verify the efficiency of the presented technique numerical and experimental tests were performed. In the first case, random field estimation of the beam flexural bending and mass per unit length have were performed. The discretized variables (ξ) were estimated from the synthetic measured FRF through a non-linear least squares curve fit procedure. A subset of these random variables can be considered as parameters to reconstruct the random field of the flexural bending and mass per unit of length. In the experimental test, an experimentally obtained FRF was used. An experimental measurement of Young's modulus at 22 points along the beam was performed using ultrasound. By comparing the reconstructed and experimentally measured of $EI(x)$ the proposed method proved to work reasonably well. Ongoing work consists of improving these preliminary results by curve fitting many measured FRF, instead of just one, to enrich the spatial information of the measured data. Based on the numerical and experimental cases presented, it was shown that the proposed method can be used to reconstruct the distributed variability of the beam. In all cases, the random field samples were reconstructed with a certain error associated. In general, all results were satisfactory, close shape of the random field sample was estimated, which demonstrated the performance of the proposed technique.

References

[1] I.M. Sobol', A Primer for the Monte Carlo Method, CRC Press, 1994.
[2] D. Xiu, Numerical Methods for Computations-A Spectral Method Approach, Princeton University Press, 2010.
[3] R. Ghanem, P. Spanos, Stochastic Finite Elements – A Spectral Approach, Sprin, 1991.
[4] G. Stefanou, The stochastic finite element method: past, present and future, Comput. Methods Appl. Mech. Eng. 198 (2009) 1031–1051.
[5] S. Adhikari, Doubly spectral stochastic finite-element method for linear structural dynamics, Am. Soc. Civ. Eng. 1 (2011) 264–276.
[6] J.F. Doyle, Wave Propagation in Structures: Spectral Analysis using Fast Discrete Fourier Transforms, second ed., Mechanical Engineering, Springer-Verlag New York, Inc., New York, 1997.
[7] U. Lee, Spectral Element Method in Structural Dynamics, BInha University Press, 2004.
[8] S.M. Hashemi, M.J. Richard, G. Dhatt, A new Dynamic Finite Element (DFE) formulation for lateral free vibrations of Euler-Bernoulli spinning beams using trigonometric shape functions, J. Sound Vib. 220 (4) (1999) 601–624.
[9] S.M. Hashemi, M.J. Richard, Free vibrational analysis of axially loaded bending-torsion coupled beams: a dynamic finite element, Comput. Struct. 77 (6) (2000) 711–724.
[10] M. Paz, Structural Dynamics: Theory and Computation, second ed., Van Nostrand, Reinhold, 1980.
[11] J.R. Banerjee, F.W. Williams, Exact Bernoulli-Euler dynamic stiffness matrix for a range of tapered beams, Int. J. Numer. Meth. Eng. 21 (12) (1985) 2289–2302.
[12] J.R. Banerjee, Coupled bending torsional dynamic stiffness matrix for beam elements, Int. J. Numer. Meth. Eng. 28 (6) (1989) 1283–1298.
[13] J.R. Banerjee, F.W. Williams, Coupled bending-torsional dynamic stiffness matrix for Timoshenko beam elements, Comput. Struct. 42 (3) (1992) 301–310.
[14] J.R. Banerjee, S.A. Fisher, Coupled bending torsional dynamic stiffness matrix for axially loaded beam elements, Int. J. Numer. Meth. Eng. 33 (4) (1992) 739–751.
[15] N.J. Ferguson, W.D. Pilkey, Literature review of variants of dynamic stiffness method, Part 1: the dynamic element method, Shock Vib. Digest 25 (2) (1993) 3–12.
[16] N.J. Ferguson, W.D. Pilkey, Literature review of variants of dynamic stiffness method, Part 2: frequency-dependent matrix and other, Shock Vib. Digest 25 (4) (1993) 3–10.
[17] J.R. Banerjee, F.W. Williams, Free-vibration of composite beams – an exact method using symbolic computation, J. Aircraft 32 (3) (1995) 636–642.
[18] C.S. Manohar, S. Adhikari, Dynamic stiffness of randomly parametered beams, Probab. Eng. Mech. 13 (1) (1998) 39–51.
[19] J.R. Banerjee, Dynamic stiffness formulation for structural elements: a general approach, Comput. Struct. 63 (1) (1997) 101–103.
[20] S. Adhikari, C.S. Manohar, Transient dynamics of stochastically parametered beams, ASCE J. Eng. Mech. 126 (11) (2000) 1131–1140.
[21] A. Papoulis, S.U. Pillai, Probability, Random Variables and Stochastic Processes, McGraw-Hill, Boston, 2002.
[22] F. Poirion, C. Soize, Monte Carlo construction of Karhunen-Loeve expansion for non-gaussian random fields, in: Proceedings of the 13th ASCE Engineering Mechanics Division Conference, 1999.
[23] P.F. Puig, B.C. Soize, Non-gaussian simulation using hermite polynomial expansion: convergences and algorithms, Probab. Eng. Mech. 17 (3) (2002) 253Dc264, https://doi.org/10.1016/S0266-8920(02)00010-3.
[24] S. Sakamoto, R. Ghanem, Simulation of multi-dimensional non-Gaussian non-stationary random fields, Probab. Eng. Mech. 17 (2) (2002) 167–176.
[25] K.K. Phoon, H.W. Huang, S.T. Quek, Simulation of strongly non-gaussian processes using Karhunen-Loeve expansion, Struct. Saf. 20 (2) (2005) 1881198, https://doi.org/10.1016/j.probengmech.2005.05.007.
[26] J.E. Mottershead, M. Friswell, Model updating in structural dynamics: a survey, J. Sound Vib. 167 (2) (1993) 347–375.
[27] M.I. Friswell, J.E. Mottershead, Finite Element Model Updating in Structural Dynamics, Kluwer Academic Publishers, 1995.
[28] M. Link, O. Santiago, Updating and localizing structural errors based on minimization of equation errors, in: International Conference on Space-craft Structures and Mechanical Testing (ESA/ESTEC), 1991.
[29] J. Mottershead, M. Friswell, G. Ng, J. Brandon, Geometric parameters for finite element model updating of joints and constraints, Mech. Syst. Signal Process. 10 (2) (1996) 171–182.
[30] G. Gladwell, H. Ahmadian, Generic element matrices suitable for finite element updating, Mech. Syst. Signal Process. 9 (6) (1996) 601–614.
[31] M.I. Friswell, J. Mottershead, H. Ahmadian, Combining subset selection and parameter constraints in model updating, ASME J. Vib. Acoust. 120 (4) (1998) 854–859.
[32] J.E. Mottershead, M. Link, M.I. Friswell, The sensitivity method in finite element model updating: a tutorial, Mech. Syst. Signal Process. 25 (2011) 2275–2296.
[33] D.J. Ewins, Modal Testing: Theory and Practice, Research Studies Press, 1984.
[34] N.M. Maia, M. Julio, Theoretical and Experimental Modal Analysis, Research Studies Pre, 1997.
[35] S. Modak, K. Kundra, B. Nakra, Prediction of dynamic characteristic using updated finite element models, J. Sound Vib. 254 (3) (2002) 447–467.
[36] M.I. Friswell, Using vibration data and statistical measures to locate damage in structures, Modal Anal. Int. J. Anal. Exp. Modal Anal. 9 (1994) 239–254.
[37] J. Mottershead, C. Mares, M. Friswell, S. James, Selection and updating of parameters for an aluminium space-frame model, Mech. Syst. Signal Process. 14 (6) (2000) 923–944, https://doi.org/10.1006/mssp.2000.1303.
[38] H. Ahmadian, J.E. Mottershead, S. James, M.I. Friswell, C.A. Reece, Modelling and updating of large surface-to-surface joints in the awe-mace structure, Mech. Syst. Signal Process. 20 (4) (2006) 868–880.
[39] N.M.M. Maia, J.M.M. Silva (Eds.), Theoretical and Experimental Modal Analysis, Engineering Dynamics Series, Research Studies Press, Taunton, England, 1997 (series Editor, J.B. Robetrs).

[40] H. Natke, Die korrektur des rechenmodells eines elastomechanischen systems mittels gemessener erzwungener schwingungen, Ingenieur-Archiv 46 (1977) 169–184.
[41] H. Natke, Updating computational models in the frequency domain based on measured data: a survey, Probab. Eng. Mech. 3 (1988) 28–35.
[42] N. Cottin, H. Felgenhauer, H.G. Natke, On the parameter identification of elastomechanical systems using inout and output residuals, Ingenieure Archiv 54 (5) (1984) 378–387.
[43] M. Link, Identification and correction of errors in analytical models using test data theoretical and practical bounds, in: International Conference on Space-craft Structures and Mechanical Testing (ESA/ESTEC), 1990.
[44] S.R. Ibrahim, W. DAmbrogio, P. Salvini, S. Sestieri, Direct updating of nonconservative finite element models using measured input-output, in: 10th International Modal Analysis Conference, San Diego, USA, 1992.
[45] H. Natke, Einfuhrung in Theorie und Praxis der Zeitreihen und Modalanalyse, Vieweg Verlag, 1992.
[46] J. Arruda, J.D. Santos, Mechanical joint parameter estimation using frequency response function and component mode synthesis, Mech. Syst. Signal Process. 7 (6) (1993) 493–508.
[47] H. Grafe, Model Updating of Large Structural Dynamics Models using Measured Response Functions (Ph.D. Thesis), Imperial College of Science, Technology and Medicine University of London Model, 1998.
[48] H.H. Khodaparast, J. Mottershead, Efficient methods in stochastic model updating, in: Proceedings of ISMA, 2008.
[49] H.H. Khodaparast, J.E. Mottershead, M.I. Friswell, Perturbation methods for the estimation of parameter variability in stochastic model updating, Mech. Syst. Signal Process. 22 (8) (2008) 1751–1773.
[50] H. Khodaparast, Stochastic Finite Element Model Updating and its Application in Aeroelasticity (Ph.D. Thesis), University of Liverpool, 2010.
[51] O.A. Vanli, S. Jung, Statistical updating of finite element model with lamb wave sensing data for damage detection problems, Mech. Syst. Signal Process. 42 (s 1–2) (2014) 137–151.
[52] Jon D. Collins, Gary C. Hart, T.K. Hasselman, B. Kennedy, Statistical identification of structures, AIAA J. 12 (2) (1974) 185–190.
[53] M.I. Friswell, The adjustment of structural parameters using a minimum variance estimator, Mech. Syst. Signal Process. 3 (1989) 143–155, https://doi.org/10.1016/0888-3270(89)90013-7.
[54] J.L. Beck, L.S. Katafygiotis, Updating models and their uncertainties. I: Bayesian statistical framework, J. Eng. Mech. 124 (4) (1998) 455–461.
[55] L.S. Katafygiotis, J.L. Beck, Updating models and their uncertainties. II: Model identifiability, J. Eng. Mech. 124 (4) (1998) 463–467.
[56] C. Mares, J.E. Mottershead, M.I. Friswell, Stochastic model updating: part 1 – theory and simulated example, Mech. Syst. Signal Process. 20 (7) (2006) 1674–1695.
[57] T. Haag, J. Herrmann, M. Hanss, Identification procedure for epistemic uncertainties using inverse fuzzy arithmetic, Mech. Syst. Signal Process. 24 (7) (2010) 2021–2034.
[58] C. Soize, Robust updating of uncertain computational models using experimental modal analysis, AIAA J. 46 (11) (2008) 2955–2965.
[59] J. Mottershead, C. Mares, S. James, M. Friswell, Stochastic model updating: Part 2: application to a set of physical structures, Mech. Syst. Signal Process. 20 (8) (2006) 2171–2185.
[60] Y. Govers, M. Link, Stochastic model updating covariance matrix adjustment from uncertain experimental modal data, Mech. Syst. Signal Process. 24 (3) (2010) 696–706, https://doi.org/10.1016/j.ymssp.2009.10.006.
[61] J. Beck, S. Au, Bayesian updating of structural models and reliability using Markov chain Monte Carlo simulation, J. Eng. Mech. 128 (4) (2002) 380–391.
[62] J.R. Fonseca, M.I. Friswell, J.E. Mottershead, A.W. Lees, Uncertainty identification by the maximum likelihood method, J. Sound Vib. 288 (3) (2005) 587–599.
[63] X. Hua, Y. Ni, Z. Chen, J. Ko, An improved perturbation method for stochastic finite element model updating, Int. J. Numer. Meth. Eng. 73 (13) (2008) 1845–1864.
[64] S. Adhikari, M. Friswell, Distributed parameter model updating using the Karhunen-Loève expansion, Mech. Syst. Signal Process. 24 (2010) 326–339.
[65] L. Meirovitch, Principles and Techniques of Vibrations, Prentice-Hal, 1997.
[66] M.I. Friswell, J.E. Mottershead, H. Ahmadian, Finite element model updating using experimental test data: parametrization and regularization, Philosoph. Trans. Roy. Soc. London Ser. A – Math. Phys. Eng. Sci. 359 (1778) (2001) 169–186.
[67] H. Ahmadian, J. Mottershead, M. Friswell, Regularisation methods for finite element model updating, Mech. Syst. Signal Process. 1 (1998) 47–64.
[68] M. Friswell, J. Mottershead, H. Ahmadian, Finite element model updating using experimental test data: parameterisation and regularisation, Trans. Roy. Soc. London, Ser. A: Math., Phys. Eng. Sci. 359 (2001) 169–186.
[69] J.E. Mottershead, C.D. Foster, On the treatment of ill-conditioning in spatial parameter estimation from measured vibration data, Mech. Syst. Signal Process. 5 (2) (1991) 139–154.
[70] B. Titurus, M. Friswell, Regularization in model updating, Int. J. Numer. Meth. Eng. 75 (2008) 440–478.
[71] M. Link, Updating of analytical models procedures and experiments, in: Conference on Modern Practice in Stress and Vibration Analysis, April 1993, pp. 35–52.
[72] R. Allemang, D. Brown, A correlation coefficient for modal vector analysis, in: 1st International Modal Analysis Conference, Orlando, USA, 1982.
[73] R. Allemang, The modal assurance criterion (mac): twenty years of use and abuse, in: IMAC-XX: Conference & Exposition on Structural Dynamics, 2002.
[74] M. Link, Updating analytical models by using local and global parameters and relaxed optimisation requirements, Mech. Syst. Signal Process. 12 (1998) 7–22.
[75] J. Arruda, Objective functions for the nonlinear curve-fit of frequency response functions, AIAA J. 30 (3) (1992) 855–857.